Adsorption (2009) 15: 254–263
DOI 10.1007/s10450-009-9177-6

Dynamics of monolayer films formed on a substrate of square symmetry

A. Patrykiejew · W. Rżysko · S. Sokołowski

Published online: 26 March 2009

Abstract The paper discusses the ground state properties and dynamics of monolayer films formed by atomic adsorbates on a square lattice, being the (100) plane of a face centered cubic crystal. The vibrations of films ordered into the commensurate $c(2 \times 2)$ as well as into the recently discovered ordered phase exhibiting a distorted Archimedean tiling of the type $(3^2.4.3.4)$ are considered. The dispersion relations and the densities of states are determined and discussed.

Keywords Monolayers · Lattice dynamics · Archimedean tiling

1 Introduction

The structure and dynamics of adsorbed layers formed on solid substrates is a subject of great interest. In particular, the properties of monolayer films on well defined surfaces of crystalline solids have been intensively studied using various experimental techniques (Dash 1975; Bruch et al. 1997, 2007), computer simulations (Abraham 1981; Patrykiejew et al. 2000) and theory (Steele 1974; Dash 1975; Bruch et al. 1997, 2007).

Much work aiming at the study of dynamical properties of adsorbed films has been done using Helium atom scattering (Mason and Williams 1984; Graham 2003; Bruch et al. 1998, 2000; Braun et al. 1998) as well as theoretical approaches (Allen et al. 1971; Hakim et al. 1988; Ramseyer et al. 1992; Bruch et al. 2007). Both experiments (Braun et al. 1998) and theory (Cardini and O'Shea 1985; Bruch 1988) have demonstrated that the dispersion curves of phonons of commensurate monolayers exhibit a gap at the Brillouin-zone center, due to a net energy contribution of the corrugation potential and the broken symmetry. On the other hand, incommensurate (floating) monolayers, which are invariant under lateral translation of the monolayer center of mass, have normal modes with vanishing frequency at the Brillouin-zone center. Another signature of surface phonons is that the frequencies of normal modes dominated by in-plane vibrations strongly depend on the magnitude and orientation of the wave vector. On the other hand, the frequencies of normal modes dominated by the out-of-plane vibrations usually show only small changes with the wave vector (Gibson and Sibener 1985).

It has been demonstrated in our earlier works (for review see Patrykiejew et al. 2000) that monolayer films formed by Lennard-Jones fluid on the (100) plane of a face centered cubic (fcc) crystal may order into solid-like phases of different structure and symmetry. The surface considered forms a square lattice of sites separated by a finite potential barrier. It has been shown that when the adatoms are large enough to exclude mutual occupation of adjacent surface potential minima and when the surface potential is sufficiently strongly corrugated, the commensurate $c(2 \times 2)$ phase is a stable state at low temperatures. On the other hand, weakly corrugated surfaces favor the formation of incommensurate (floating) phase of hexagonal symmetry, in particular, for large misfit between the size of surface lattice and the diameter of adatoms.

Recently (Patrykiejew and Sokołowski 2007a, 2007b; Rżysko et al. 2008) we have also found a new type of ordered solid-like phase, in which the adatoms form a pattern being a distorted Archimedean tiling (AT) of the type

A. Patrykiejew (✉) · W. Rżysko · S. Sokołowski
Department for the Modelling of Physico-Chemical Processes, MCS University, 20031 Lublin, Poland
e-mail: andrzej@pluto.umcs.lublin.pl

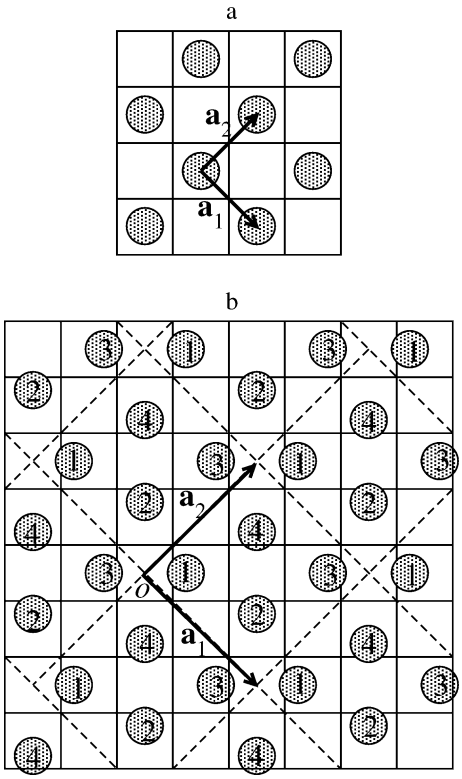

Fig. 1 Part **a** shows the commensurate $c(2 \times 2)$ structure, while part **b** the AT structure. Note that unit cell of AT phase contains four atoms in nonequivalent positions

$(3^2,4,3,4)$ (Grünbaum and Shepard 1987; Schmiedeberg and Stark 2008; Patrykiejew and Sokołowski 2008). The notation $(3^2,4,3,4)$ reflects the shape of the unit cell consisting of a sequence of triangles and squares (cf. Fig. 2b). In order to establish the regime of parameters (misfit between adatoms and the surface lattice, surface potential strength and corrugation and temperature) over which the monolayer films are likely to order into the AT phase, extensive Monte Carlo simulation has been carried out (Rżysko et al. 2008).

The aim of this paper is to determine the dynamics of monolayer solid-like films ordered into the AT phase. We discuss the dispersion relations for the commensurate $c(2 \times 2)$ phase, for the AT structures developing from the $c(2 \times 2)$ structure and for the floating monolayer of hexagonal symmetry.

2 Theoretical background

In general, when the monolayer film formed on a crystal surface orders into a periodic superstructure, its unit cell is characterized by two vectors $\boldsymbol{a}_1$ and $\boldsymbol{a}_2$ and contains n atoms. In the case of a simple commensurate $c(2 \times 2)$ structure, the unit vectors are equal to $\boldsymbol{a}_1 = a(1, 1)$ and $\boldsymbol{a}_2 = a(1, -1)$ (a being the surface lattice spacing) and the unit cell contains only one atom (see Fig. 1a). On the other hand, the AT

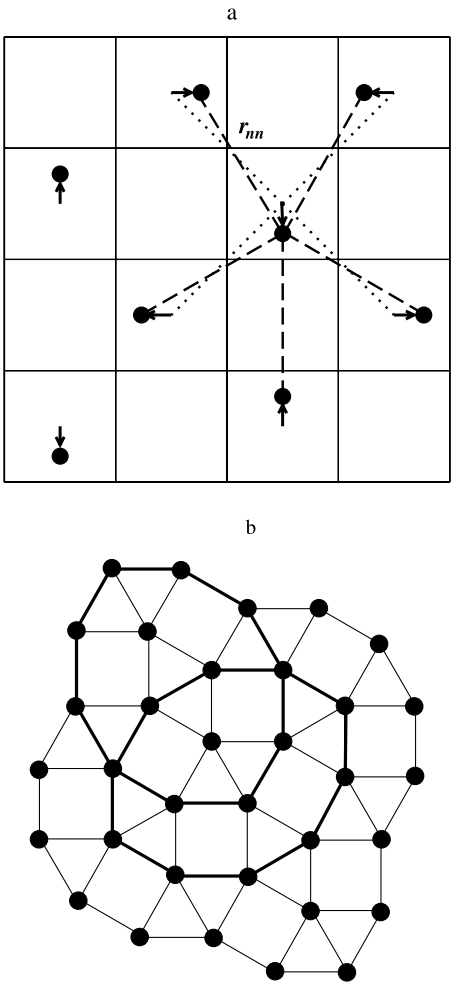

Fig. 2 Part **a** represents a basic 4×4 unit lattice allowing to construct AT phase on a square lattice from the commensurate $c(2 \times 2)$ phase. The *arrows* show the displacement vectors applied to all atoms. *Dotted and dashed lines* represent the nearest neighbor distances in the commensurate and in the AT ordered phases, respectively. Part **b** shows a perfect AT order with the tiling observed in snapshots recorded during simulation runs

ordered structure has larger unit cell, characterized by the vectors $\boldsymbol{a}_1 = a(2, 2)$ and $\boldsymbol{a}_2 = a(2, -2)$, and contains four atoms (see Fig. 1b). It has been demonstrated (Patrykiejew and Sokołowski 2008; Rżysko et al. 2008) that the AT structure develops from the commensurate $c(2 \times 2)$ phase by the displacement of adsorbate atoms from registry positions in a manner shown in Fig. 2a. The displacement of each adatom from its registry position takes place only along one of the surface lattice symmetry axes and the displacement vectors for all atoms have the same length (Δ_m). In the resulting structure every adatom has five nearest neighbors and in an idealized situation, in which all nearest neighbor distances are the same ($\Delta_o = (\sqrt{3}-1)/(\sqrt{3}+1) \approx 0.2679$ and $r_{nn} = 4/(\sqrt{3}+1) \approx 1.464$), we obtain the pattern like that shown in Fig. 2b, being a perfect Archimedean tiling of the type $(3^2.4.3.4)$. Both Monte Carlo simulation as well as the

ground state calculations have shown (Rżysko et al. 2008), however, that the displacement vectors in adsorbed films are smaller than Δ_o and the tiling is not perfect. This is due to the competing effects of adatom-adatom and adatom-surface interactions.

Now, let

$$\boldsymbol{r}_o(l,s) = \boldsymbol{R}(l) + \boldsymbol{\tau}(s) + z(s) \tag{1}$$

be the equilibrium position of the s-th atom in the l-th unit cell. In the above equation $\boldsymbol{R}(l) = l_1\boldsymbol{a}_1 + l_2\boldsymbol{a}_2$ (l_1 and l_2 being integers) specifies the position of the l-th unit cell, $\boldsymbol{\tau}(s)$ gives the lateral position of the s-th atom within a unit cell and $z(s)$ is the distance of the s-th atom from the surface.

The positions of atoms within a unit cell of the AT phase are specified by the vectors $\boldsymbol{\tau}(s)$ (measured with respect to the point marked by o in Fig. 1b) given by

$$\begin{aligned} &\boldsymbol{\tau}(1) = (1.0 - \Delta_m, 0), \qquad \boldsymbol{\tau}(2) = (2, -1.0 + \Delta_m), \\ &\boldsymbol{\tau}(3) = (3.0 + \Delta_m, 0), \qquad \boldsymbol{\tau}(4) = (2, 1.0 - \Delta_m). \end{aligned} \tag{2}$$

One should note that the registry position corresponds to the center of the surface lattice unit cell, given by $\boldsymbol{\tau}_c = (0.5, 0.5)$. Since the displacements of atoms from registry positions take place only along one of the surface lattice symmetry axes and all have the same length (Δ_m), all atoms within a super-cell are placed at the same distance form the surface, $z(s) = z_m$

Now, we assume that the interaction between a pair of adsorbate atoms is represented by the Lennard-Jones potential

$$u(r) = 4\varepsilon[(\sigma/r)^{12} - (\sigma/r)^6]. \tag{3}$$

Also, the adatoms are assumed to interact with the substrate atoms via the Lennard-Jones potential. The substrate surface is a square lattice of sites and we take the length of the surface lattice constant a as a unit of length and ε is used as a unit of energy.

Assuming further that the substrate is rigid, the surface field, being periodic in the directions parallel to the surface (x and y), can be represented by the Fourier series (Steele 1973)

$$v^*(z^*, \boldsymbol{\tau}^*) = \varepsilon^*_{gs}\left[v_o(z^*) + V_b \sum_{g\neq 0} v_g(z^*) f_g(\boldsymbol{\tau}^*)\right], \tag{4}$$

where $z^* = z/a$ is the distance from the surface, $\boldsymbol{\tau}^* = (x^*, y^*)$ ($x^* = x/a$ and $y^* = y/a$) is the 2D vector specifying the position of an adatom over the surface lattice and the sum runs over different (non-zero) reciprocal surface lattice vectors. The Fourier coefficients $v_g(z^*)$ and the functions $f_g(\boldsymbol{\tau}^*)$ are given by analytic expressions (Steele 1973). The parameter V_b has been introduced in order to allow for changes of the periodic part of the surface potential (Kim and Steele 1992). As long as the parameter V_b is equal to unity and provided that a sufficient number of terms in the sum over reciprocal lattice vectors has been taken into account, the Fourier series (4) gives the same values of the adatom-substrate interaction energies as a direct summation of interactions between the adatom and the atoms of semi-infinite substrate. In the case of the surface being the (100) plane of an fcc crystal considered here, it is sufficient to use the first five non-zero reciprocal lattice vectors.

The total potential energy for the monolayer is a sum of contributions due to the adatom-adatom and the adatom-substrate interactions

$$U = U_{a-a} + V_{a-s} = \frac{1}{2}\sum_{lsl's'} u(r_{lsl's'}) + \sum_{ls} v[\boldsymbol{r}(l,s)]. \tag{5}$$

In the harmonic approximation, we can write

$$\begin{aligned} U = U_o + \frac{1}{2}\sum_{\alpha,\beta}\sum_{lsl's'} &[\Psi_{\alpha\beta}(lsl's') \\ &+ \Phi_{\alpha\beta}(ls)\delta_{ll'}\delta_{ss'}]u_\alpha(ls)u_\beta(l's')], \end{aligned} \tag{6}$$

where the force constants

$$\Psi_{\alpha\beta}(lsl's') = \left[\frac{\partial^2 U_{a-a}}{\partial u_(ls)\alpha u_(l's')\beta}\right]_o \tag{7}$$

and

$$\Phi_{\alpha\beta}(ls) = \left[\frac{\partial^2 U_{a-s}}{\partial u_\alpha(ls) u_\beta(ls)}\right]_o \tag{8}$$

are calculated for the equilibrium geometry of the monolayer and $\boldsymbol{u}(ls) = [u_x(ls), u_y(ls), u_z(ls)]$ is the dynamical displacement of the atom from its equilibrium position

$$\boldsymbol{u}(ls) = \boldsymbol{r}(ls) - \boldsymbol{r}_o(ls), \tag{9}$$

where the instantaneous position of the atom is represented by the vector $\boldsymbol{r}(ls)$.

The equations of motion for the displacements $\boldsymbol{u}(ls)$ are given by

$$\begin{aligned} m\frac{\partial^2 u_\alpha(ls)}{\partial t^2} = -\frac{\partial U}{\partial u_\alpha(ls)} = -\sum_{l's'\beta} &[\Psi_{\alpha\beta}(lsl's') \\ &+ \Phi_{\alpha\beta}(ls)\delta_{ll'}\delta_{ss'}]u_\beta(l's')], \end{aligned} \tag{10}$$

where m denotes the mass of adsorbate atoms, taken as equal to unity.

Exploiting translational periodicity parallel to the surface plane, the displacements are then assumed to have the form

$$u_\alpha(ls) = m^{-1/2}\epsilon_\alpha(s, \boldsymbol{k}_\parallel)\exp[i\boldsymbol{k}_\parallel \cdot \boldsymbol{R}(l) - i\omega(\boldsymbol{k}_\parallel t)], \tag{11}$$

where $\boldsymbol{k}_\parallel$ is the two-dimensional wave vector and $\epsilon_\alpha(s, \boldsymbol{k}_\parallel))$ denotes the component α of the eigenvector corresponding

to the vibrational mode. The vibration frequencies, $\omega(\boldsymbol{k}_\parallel)$, and the corresponding eigenvectors, $\boldsymbol{\epsilon}(s, \boldsymbol{k}_\parallel)$, are obtained from the set of equations:

$$\omega^2(\boldsymbol{k}_\parallel)\epsilon_\alpha(s, \boldsymbol{k}_\parallel) = \sum_{s'\beta} D_{\alpha\beta}(s, s', \boldsymbol{k}_\parallel)\epsilon_\beta(s', \boldsymbol{k}_\parallel), \tag{12}$$

where the dynamical matrix elements $D_{\alpha\beta}(s, s', \boldsymbol{k}_\parallel)$ are given by

$$D_{\alpha\beta}(s, s', \boldsymbol{k}_\parallel) = m^{-1} \sum_{l'} [\Psi_{\alpha\beta}(lsl's') \times \exp[i\boldsymbol{k}_\parallel \cdot [\boldsymbol{R}(l') - \boldsymbol{R}(l)]] + \Phi_{\alpha\beta}(ls)]. \tag{13}$$

Having the solution of (12) the density of states for vibrational modes can be readily calculated, using the relation

$$g(\omega) = (3nN)^{-1} \sum_{\boldsymbol{k}_\parallel, \gamma} \delta(\omega - \omega_\gamma(\boldsymbol{k}_\parallel)), \tag{14}$$

where $3nN$ is the number of vibrational modes and γ denotes differently polarized modes (γ runs from 1 to $3n$) Here, $n = 1$ for the commensurate $c(2 \times 2)$ and the floating incommensurate phases and $n = 4$ in the case of AT phase. The density of states gives the information about the vibrational spectrum of adsorbed layer.

In the case of the commensurate $c(2 \times 2)$ structure, the reciprocal lattice vectors of the first Brillouin zone are given by

$$\boldsymbol{k}_1 = \frac{\pi}{a}(1, -1) \quad \text{and} \quad \boldsymbol{k}_2 = \frac{\pi}{a}(1, 1) \tag{15}$$

while in the case of the AT structure these vectors are equal to

$$\boldsymbol{k}_1 = \frac{\pi}{2a}(1, -1) \quad \text{and} \quad \boldsymbol{k}_2 = \frac{\pi}{2a}(1, 1). \tag{16}$$

When the films forms an incommensurate (floating) structure of hexagonal symmetry, the unit lattice vectors are equal to $\boldsymbol{a}_1 = r_{nn}(1, 0)$ and $\boldsymbol{a}_2 = r_{nn}(-0.5, \sqrt{3}/2)$ and hence the reciprocal lattice vectors are given by

$$\boldsymbol{k}_1 = \frac{2\pi}{r_{nn}}(1, 1/\sqrt{3}) \quad \text{and} \quad \boldsymbol{k}_2 = \frac{2\pi}{r_{nn}}(0, 2/\sqrt{3}), \tag{17}$$

where r_{nn} is the nearest neighbor distance.

3 Results and discussion

From the results of Monte Carlo simulation and ground state calculations (Rżysko et al. 2008), it follows that the ordered AT structure is stable at $T = 0$ over a rather wide range of parameters σ^*, ε^*_{gs} and V_b. As we have already mentioned, the length of displacement vector, Δ_m, is lower than the value corresponding to a perfect Archimedean tiling of the type (3^2.4.3.4). Figure 3 gives the examples of ground state calculations, which demonstrate the above statement and show that the stable structure changes with the model parameters. The systems with σ^* between 1.34 and 1.36 order into the commensurate $c(2 \times 2)$ structure in the ground state. Then, in the case of $\sigma^* = 1.37$ and 1.38 the structure of the lowest energy corresponds to the AT phase. One should note, however, that the stability of the AT phase strongly depends on the parameters of the surface potential. In particular, the increase of the product $V_b\varepsilon^*_{gs}$ enhances the stability of the commensurate $c(2 \times 2)$ phase. On the other hand, when the product $V_b\varepsilon^*_{gs}$ becomes low enough, the stable state of the film corresponds to the floating incommensurate phase of triangular symmetry. This is a direct consequence of the changes in the surface potential curvatures in the directions x and y (being the same due to the symmetry properties of the lattice) (Rżysko et al. 2008). Of course, the length of displacement vectors Δ_m that minimizes the energy is different in both cases. Also, the equilibrium distance of adatoms from the surface, z^*_m, changes. For $\sigma^* = 1.37$ we have $z^*_m = 1.112$, while for $\sigma^* = 1.38$, $z^*_m = 1.119$.

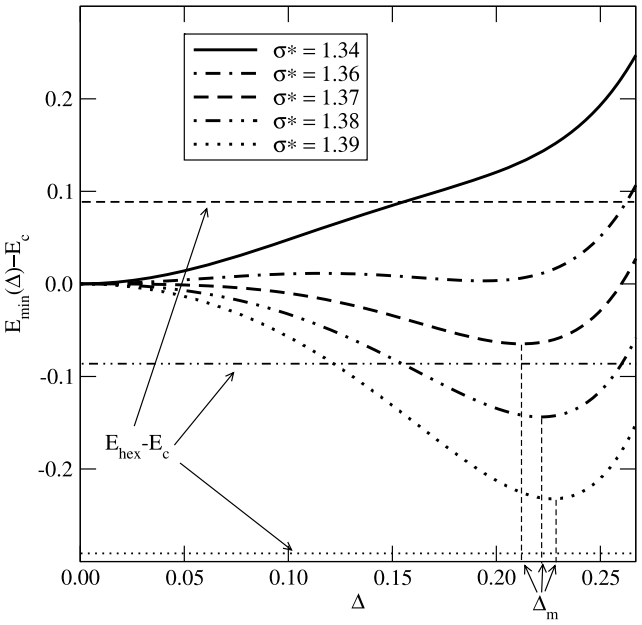

Fig. 3 The difference between the potential energies of the distorted AT phase ($E_{\min}(\Delta)$) and of the commensurate phase E_c versus Δ for a series of systems characterized by different σ^* (shown in the figure) and the surface potential with $\varepsilon^*_{gs} = 1.0$ and $V_b = 1.0$. The *horizontal lines* correspond to the differences between the energies of hexagonal floating and the commensurate films

One should also take into account the possibility that the film forms incommensurate floating phase of hexagonal symmetry. The calculation of the ground state energy of such an incommensurate phase is a nontrivial task. The

corrugation potential is expected to cause distortions of a perfect hexagonal symmetry and may also lead to the so-called epitaxial rotation (Novaco and McTague 1977; McTague and Novaco 1979; Leatherman et al. 1997). Here, we neglect those complexities and assume that the incommensurate phase forms a perfectly ordered hexagonal lattice. Under such assumption, the ground state calculations demonstrate that in the case of the systems shown in Fig. 3, the floating phase has higher energy than the AT phase for $\sigma^* \leq 1.38$. When, however, we assume that $\sigma^* = 1.39$, the floating incommensurate phase has lower energy than the AT phase. Therefore, it is expected that the system with $\sigma^* = 1.39$ forms a hexagonally ordered phase at low temperatures. This has been confirmed by Monte Carlo simulation (Rżysko et al. 2008).

We begin with the discussion of systems ordering into the commensurate $c(2 \times 2)$ structure at low temperatures and consider two series of systems. The first series corresponds to monolayers formed by atoms of different size, σ^*, ranging between 1.20 and 1.36, under the condition of fixed $\varepsilon^*_{gs} = 1.0$ and $V_b = 1.0$.

Figure 4 presents the dispersion curves for a the systems of different size of adatoms. The modes propagating in the film can be characterized by its orientation with respect to the plane defined by the vectors $\boldsymbol{k}_\parallel$ and the vector $\boldsymbol{n}$, normal to the surface, called the sagittal plane (de Rouffignac et al. 1981). For a given $\boldsymbol{k}_\parallel$ the vibration modes are labelled by their dominant polarization. The modes with the dominating displacements in the sagittal plane are labelled as $SP_\parallel$ and $SP_\perp$, and correspond to the displacements parallel and perpendicular to the wave vector $\boldsymbol{k}_\parallel$, respectively. The mode with the displacement normal to the sagittal plane is labelled as SH (shear horizontal).

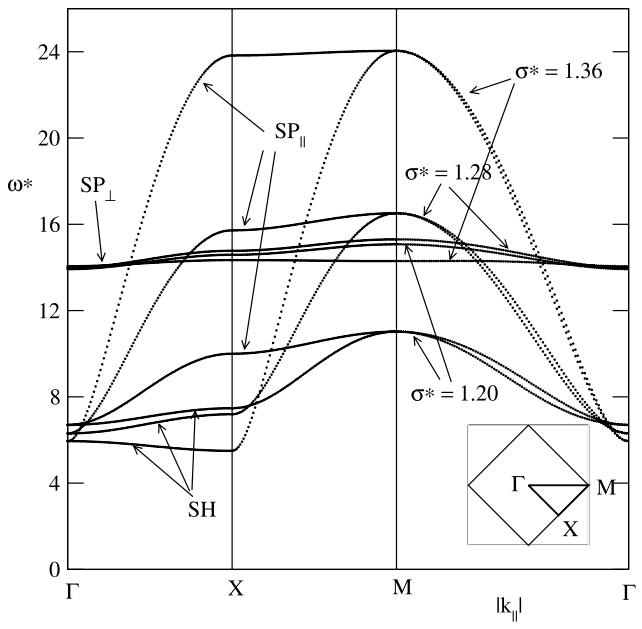

Fig. 4 The dispersion relations for the commensurate $c(2 \times 2)$ phase for the systems characterized with $\varepsilon^*_{gs} = 1.0$, $V_b = 1.0$ and different σ^* (shown in the figure)

One readily notes that the optical branch, corresponding to the $SP_\perp$ mode, is nearly non-dispersive and only very slightly affected by the change of σ^*. This results from rather weak dependence of the force constant Φ_{zz} on σ^* and small values of the force constant Ψ_{zz}. On the other hand, the two acoustic branches, dominated by the in-plane vibrations, exhibit pronounced changes with σ^*. Of course, the normal mode frequencies for the in-plane vibrations have nonzero values at the Brillouin-zone center, as expected for the commensurate monolayer (Cardini and O'Shea 1985; Bruch 1988). The zone-center gap for vibrations can be readily obtained by taking into account that it is entirely determined by the corrugation potential and using the following equation

$$\omega_o = (\Phi_{xx}/m)^{1/2}, \tag{18}$$

where Φ_{xx} depends on the periodic part of the surface potential only.

The dispersion relations also demonstrate that the two acoustic modes become degenerate as $\boldsymbol{k}_\parallel$ approaches the center of the Brillouin zone, due to the symmetry properties of the corrugation potential. It is also evident that the two in-plane modes strongly depend on the diameter of adatoms, as well as on the orientation of the wave vector. In all cases, the vibration frequencies of $SP_\parallel$ and SH modes are nearly the same for the wave vector running along the Γ-M direction. On the other hand, they are quite different for the wave vectors along the M-X as well as along X-Γ directions. A strong increase of both frequencies with σ^* for the wave vector oriented along the Γ-M direction as well as of the $SP_\parallel$ mode along the M-X direction are associated with the changes in the force constants of the adatom-adatom interaction potential, when the film becomes more and more compressed.

Figure 5 presents the density of states, $g(\omega*)$, obtained for the same systems as presented in Fig. 4, and normalized to unity, i.e.,

$$\int g(\omega*) = 1.0. \tag{19}$$

The obtained spectra indicate the changes in the vibration frequencies when the misfit between adatoms and the surface lattice increases. In the case of $\sigma^* = 1.20$, a rather large gap, separating the frequency regions of SH and $SP_\parallel$ vibrations from the $SP_\perp$ vibrations occurs. This gap is, of course, not present in the spectra obtained for $\sigma^* = 1.28$ and 1.36. In the case of $\sigma^* = 1.36$, the $SP_\perp$ mode is nearly independent of the wave vector, and hence it produces very sharp peak, while the two other peaks, at $\omega^* \approx 6$ and 23.8, exhibit very low relative intensities.

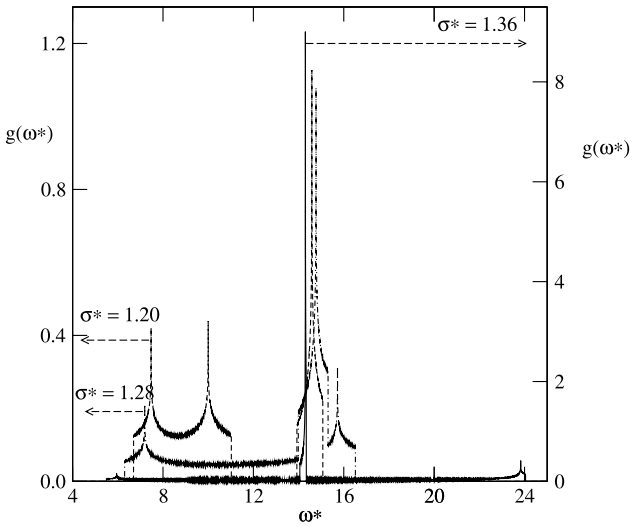

Fig. 5 The histograms $g(\omega^*)$ for the same systems as in Fig. 3

One also expects that the normal mode frequencies should depend on the properties of the adatom-surface interaction potential. In particular, for the fixed σ^*, the zone-center frequency gap for the acoustic modes should increase with ε^*_{gs} (for the fixed V_b) and decrease when the corrugation parameter decreases, while ε^*_{gs} is kept constant. This is a consequence of the fact that the force constants $\Phi_{\alpha\beta}(ls)$, for $\alpha = x, y$ and $\beta = x, y$ are proportional to the product $\varepsilon^*_{gs} V_b$. On the other hand, the frequency of the optical branch is expected to increase with ε^*_{gs}, but to be only weakly affected by the magnitude of the corrugation parameter. The force constant $\Phi_{zz}(ls)$ has the form

$$\Phi_{zz}(ls) = \varepsilon^*_{gs}\left[\left(\frac{\partial^2 v_o(z^*)}{\partial z^2}\right)_o + V_b \sum_{g\neq 0}\left(\frac{\partial^2 v_g(z^*)}{\partial z^2}\right)_o f_g(\boldsymbol{\tau}^*)\right] \quad (20)$$

and it was demonstrated (Rżysko et al. 2008) that the first term is dominating and the contribution due to the second term does not exceed 5%. Moreover, the contribution due to the periodic part of the surface potential is not a monotonous function of the corrugation parameter.

The above predictions are illustrated by the results shown in Fig. 6. In part a of Fig. 6, we show examples of dispersion relations for the systems characterized by $\sigma^* = 1.41$, $V_b = 1.0$ and different ε^*_{gs}, while part b of Fig. 6 presents the dispersion relations for the systems with $\sigma^* = 1.40$, $\varepsilon^*_{gs} = 5.0$ and for different values of the corrugation parameter V_b.

The data presented in Fig. 6a show that the frequencies of the normal modes increase withε^*_{gs} as expected. Also the zone center frequency gap for $SP_{\parallel}$ and SH normal modes is considerably affected by the magnitude of ε^*_{gs}.

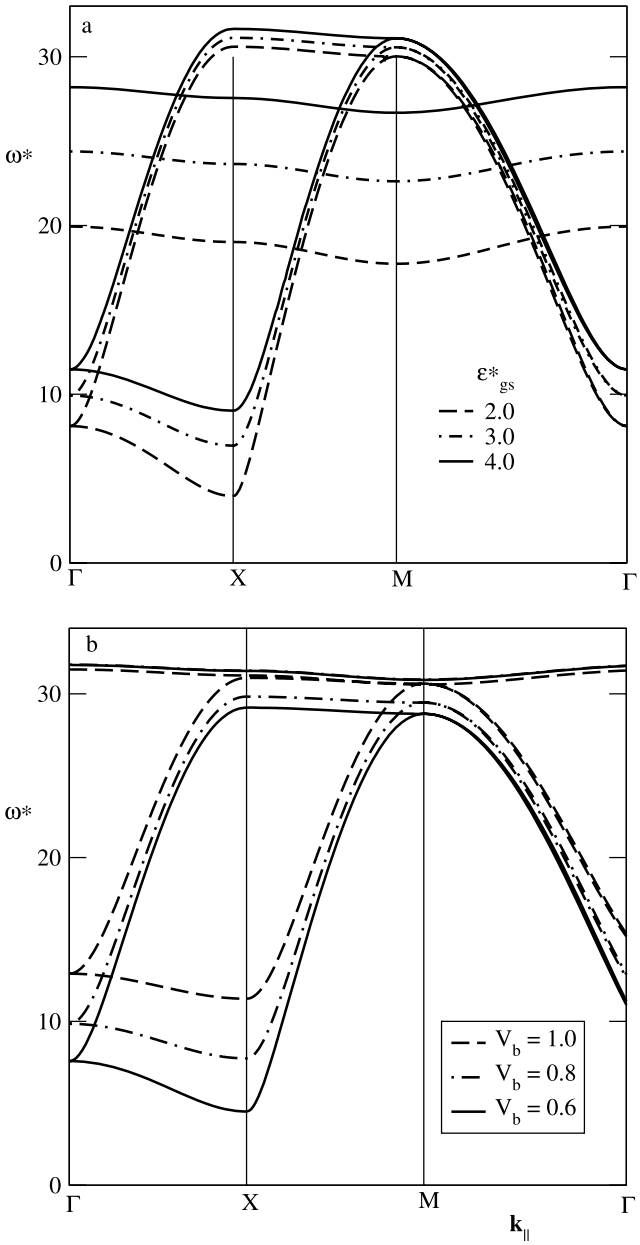

Fig. 6 Part **a** shows the dispersion relations for the commensurate $c(2\times 2)$ phase for the systems characterized with $\sigma^* = 1.41$, $V_b = 1.0$ and different values of ε^*_{gs} (shown in the figure), while part **b** shows the dispersion relations for the commensurate $c(2\times 2)$ phase for the systems characterized with $\sigma^* = 1.40$, $\varepsilon^*_{gs} = 5.0$ and different values of V_b (shown in the figure)

The results given in Fig. 6b are also consistent with the above discussion. Thus, the zone-center frequency gap decreases when the corrugation parameter is lowered, while the frequency of the $SP_{\perp}$ mode is only very weakly affected by the magnitude of the parameter V_b.

Now, we present the results obtained for the AT structure. Figure 7 presents the dispersion curves for the system with $\sigma^* = 1.37$, $\varepsilon^*_{gs} = 1.0$ and $V_b = 1.0$. Calculations for other systems ordering into the AT phase have given qualitatively

similar results. The classification of normal modes is not so simple as in the case of commensurate film with only one atom per unit cell. Nonetheless, the recorded eigenvectors at selected points over the first Brillouin zone (a representative example obtained for the vector $\boldsymbol{k}_{\parallel}$ corresponding to the X point is given in Table 1) allow to classify normal modes with respect to dominating amplitudes of displacements in different directions. Thus, the modes labelled as 1, 2, 3 and 6 can be considered as analogous to the SH mode of the commensurate film, as the largest amplitudes correspond to the direction perpendicular to the sagittal plane. The remaining modes are the combinations of $SP_{\perp}$ and $SP_{\parallel}$ vibrations. In different modes, the pairs of atoms 1, 3 and 2, 4 show similar displacements. The calculations for various systems allow us to state that the modes 5, 8, 10 and 12 are dominated by the vibrations normal to the surface, thus are most like the $SP_{\perp}$ vibrations, while the modes 4, 7, 9 and 11 are analogs of the $SP_{\parallel}$ modes, though they involve quite large displacements of two atoms in the direction normal to the surface.

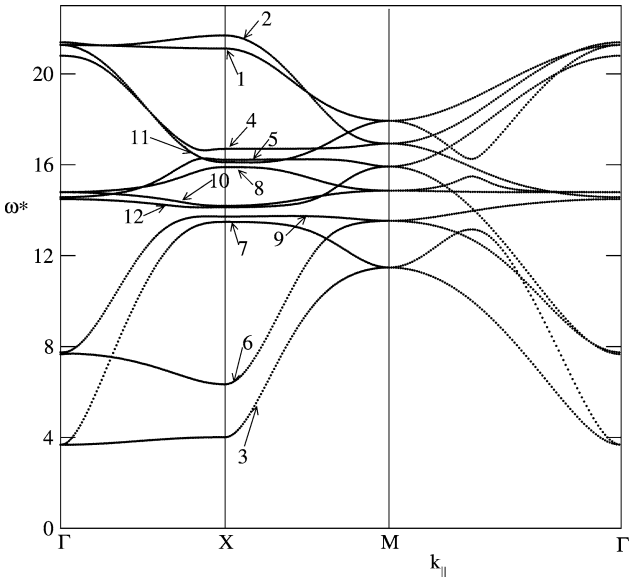

Fig. 7 The dispersion relations for the AT phase for the system characterized by $\varepsilon^*_{gs} = 1.0$, $V_b = 1.0$ and $\sigma^* = 1.37$

Figure 8 shows the dispersion curves for two systems of adatoms with $\sigma^* = 1.38$ and different parameters characterizing the strength of surface potential: $\varepsilon^*_{gs} = 1.0$ (part a) and 1.2 (part b), with the fixed $V_b = 1.0$. The assignment of modes is quite the same as in the previously presented case. We note that the vibration frequencies of the modes 5, 8, 10 and 12 increase with ε^*_{gs}, as predicted for the modes dominated by the vibrations normal to the surface. Also, we observe a small increase of the zone-center gap.

Figure 9 gives the normalized to unity density of states for the same system as shown in Fig. 8. The spectrum is considerably more complex than that of the commensurate monolayer films (see Fig. 5). The first region of the spectrum, corresponding to ω^* up to about 14.0, corresponds to the modes 3, 6, 7 and 9 modes. Then, we have sharp signals associated with the vibrations dominated by the out of plane displacement (the modes: 5, 8, 10 and 12) which partially overlap with the signals due to the modes 4 and 11. The high energy peaks, which appear for ω^* close to 21, are due to the modes 1, 2, 4 and 11. In the case of the systems

Table 1 The frequencies and eigenvectors of normal modes for the system with $\sigma^* = 1.37$, $\varepsilon^*_{gs} = 1.0$ and $V_b = 1.0$, corresponding to the X position over the first Brillouin zone. The first column ($s\alpha$) labels displacements of each atom (s) along different axes (α). The atoms with a unit cell are numbered in a way shown in Fig. 1, and the mode numbers are the same as in Fig. 8

No.	1	2	3	4	5	6	7	8	9	10	11	12
ω^*	21.107	21.686	4.009	16.698	16.216	6.346	13.483	15.888	13.718	14.184	16.106	14.127
$s\alpha$	eigenvectors											
$1x$	0.4047	0.2857	−0.4362	0.4999	0.1216	−0.2664	0.1232	−0.2856	−0.2789	−0.1786	0.1308	0.0712
$1y$	0.2781	0.4000	−0.2458	−0.3044	−0.1604	−0.4109	−0.0395	0.4705	0.2098	0.3420	−0.1498	0.0929
$1z$	0.0817	0.0513	0.1008	0.3196	0.1298	0.0754	−0.0855	−0.3869	0.6107	0.5644	0.0853	0.0106
$2x$	−0.4248	0.2529	−0.3853	0.1523	−0.5209	0.2688	0.2534	−0.1128	−0.0203	0.1345	−0.2755	−0.2627
$2y$	−0.2613	0.4314	−0.2922	−0.1612	0.3090	0.4118	−0.3942	0.0860	−0.0709	0.0247	0.42760	0.1341
$2z$	0.0534	−0.0762	−0.0690	0.0809	−0.2748	0.1133	−0.5067	−0.1645	0.0020	−0.1229	−0.4417	0.6306
$3x$	0.4053	−0.2856	−0.4366	−0.4992	−0.1220	0.2663	0.1222	−0.2858	0.2790	−0.1773	0.1309	−0.0740
$3y$	0.2777	−0.4003	−0.2454	0.3048	0.1615	0.4113	−0.0385	0.4700	−0.2101	0.3433	−0.1495	−0.0870
$3z$	−0.0818	0.0513	−0.1009	0.3192	0.1298	0.0754	0.0826	0.3873	0.6104	−0.5652	−0.0848	0.0000
$4x$	−0.4258	−0.2522	−0.3862	−0.1520	0.5204	−0.2680	0.2537	−0.1133	0.0217	0.1297	−0.2752	0.2648
$4y$	−0.2615	−0.4312	−0.2925	0.1609	−0.3097	−0.4117	−.3945	0.0862	0.0687	0.0274	0.4271	−0.1338
$4z$	−0.0538	−0.0762	0.0691	0.0810	−0.2754	0.1132	0.5064	0.1652	0.0041	0.1117	0.4411	0.6329

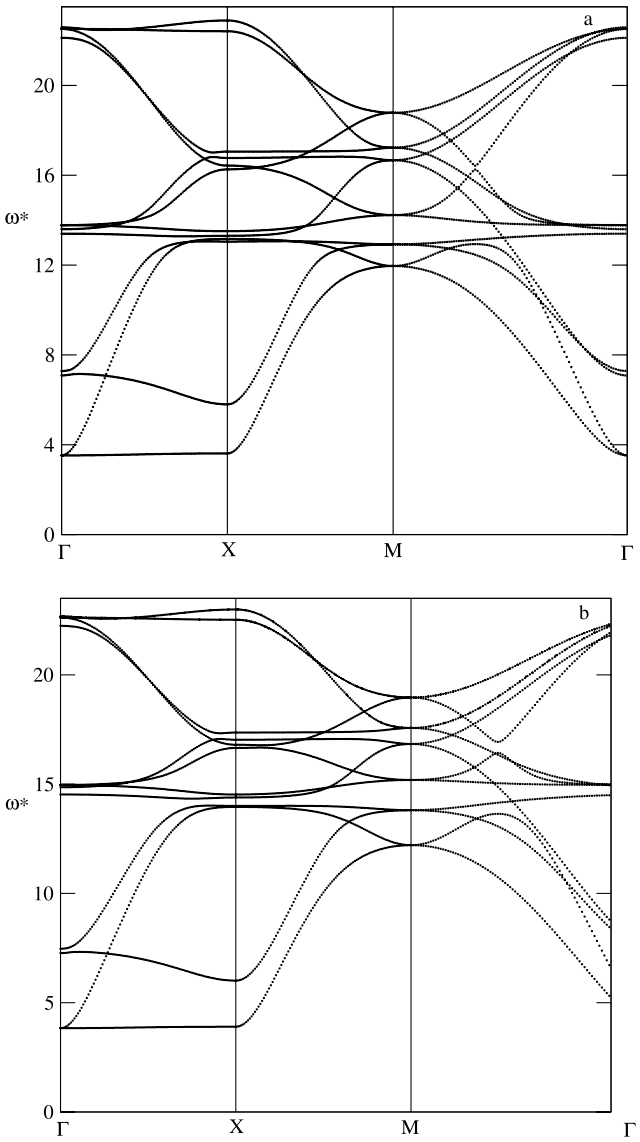

Fig. 8 The dispersion relations for the AT phase for the systems characterized by $\sigma^* = 1.38$, $V_b = 1.0$ and $\varepsilon^*_{gs} = 1.0$ (part **a**) and 1.2 (part **b**)

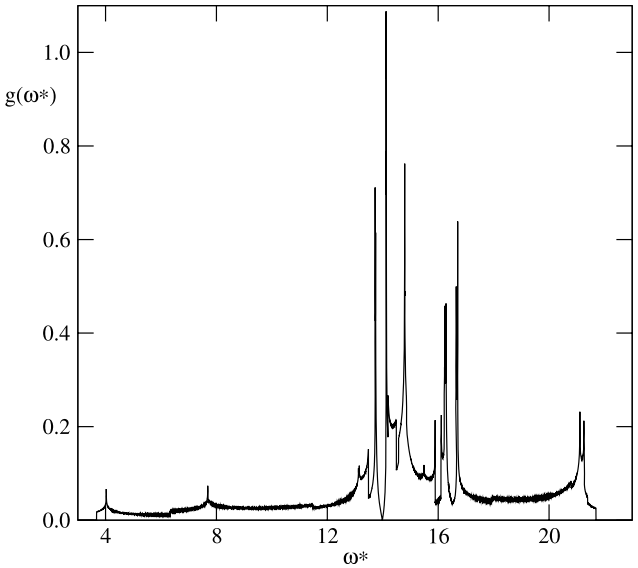

Fig. 9 The histogram $g(\omega^*)$ for the system with $\sigma^* = 1.37$, $\varepsilon^*_{gs} = 1.0$ and $V_b = 1.0$

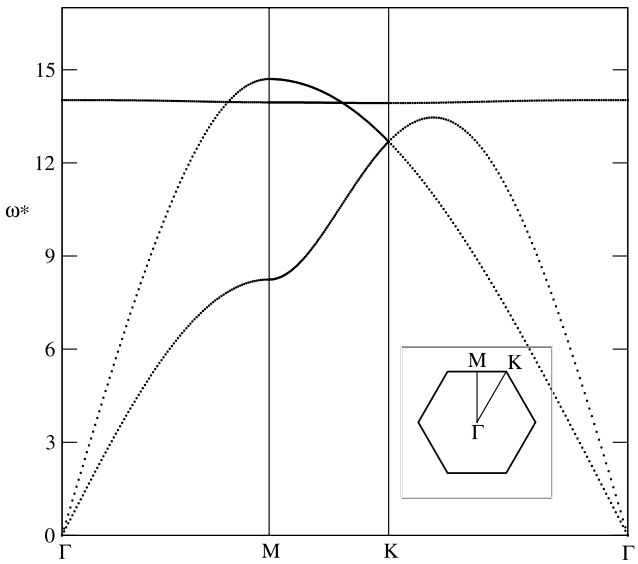

Fig. 10 The dispersion curves for the floating hexagonal monolayer formed by atoms of $\sigma^* = 1.39$ and the surface potential with $\varepsilon^*_{gs} = 1.0$ and $V_b = 1.0$

with $\sigma^* = 1.38$ (see Fig. 8), the corresponding spectra are qualitatively similar.

When the parameters of the model change, the monolayer forms a floating incommensurate phase of hexagonal symmetry. In particular, this is expected to happen when adatoms of $\sigma^* = 1.39$ are adsorbed on the surface with the potential characterized by $\varepsilon^*_{gs} = 1.0$ and $V_b = 1.0$ (see Fig. 3). Assuming that the floating phase forms a perfect hexagonal lattice, the dispersion curves look like those presented in Fig. 10. It should be noted, however, that the analysis of configurations recorded during Monte Carlo simulation has demonstrated that the hexagonally ordered phase is rotated with respect to the surface symmetry axes by a temperature dependent angle and that the unit lattice cell of the monolayer is more or less uniformly distorted along one of its symmetry axes as schematically shown in Fig. 11. The effects of uniform distortion of hexagonally ordered films on vibrational modes was discussed by Antsygina et al. (2002). It was shown that the distortion only slightly influences the frequencies of vibrations. In our calculations we have neglected such effects and hence the results given in Fig. 11 were obtained for a perfectly ordered hexagonal floating phase. Of course, the dispersion curves for the in-plane (acoustic) vibrations depicted in Fig. 9 are qualitatively the same as obtained for two dimensional systems of hexagonal symmetry (Phillips and Bruch 1979). The op-

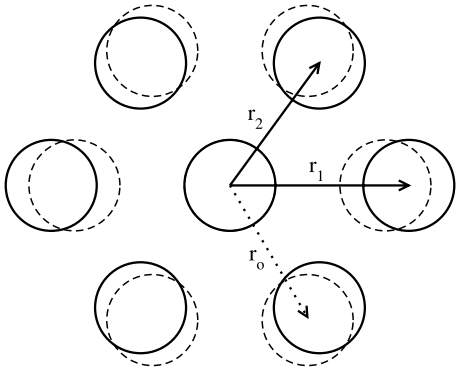

Fig. 11 Schematic picture of a uniformly distorted hexagonal lattice. A perfectly ordered hexagonal lattice is marked by circles drawn with dashed lines and the nearest neighbor distance equals to r_o. In the case of uniformly distorted lattice there are two different nearest neighbor distances: r_1 and r_2

tical branch, corresponding to the vibrations normal to the surface, is nearly non-dispersed as expected.

4 Summary

The dynamics of monolayer films on the (100) plane of a face centered cubic crystal and ordered into the commensurate $c(2 \times 2)$ as well as into the novel AT-like structures are discussed within the harmonic approximation. The dispersion curves have been determined and different vibrational modes identified. The commensurate phase has three normal modes. Two of them are acoustic and correspond to in-plane vibrations and one optical mode is due to out-of plane vibrations. The eigenvectors associated with different modes indicate that the in-plane and out of plane modes are well separated. In particular, for the in-plane modes the amplitudes of atomic displacement in the direction normal to the surface is very close to zero, while in the case of the out-of plane mode, the displacements in the plane parallel to the surface are very small. Of course, the acoustic branches exhibit the frequency gap at the Brillouin zone center.

In the case of AT phase, the unit cell contains four atoms and hence there are twelve normal modes. Again, there are acoustic as well as optical modes. Of course, each normal mode involves simultaneous displacements of all atoms and the identification of differently polarized modes is not so simple.

Concluding we would like to address the question of possible realization of AT ordering in real systems. The hitherto published experimental data for monolayer films formed on substrates of square symmetry have never demonstrated the formation of AT phase. It should be emphasized that the appearance of AT phase has been found only when the misfit between adsorbate atoms and surface lattice as well as the corrugation of surface potential are suitably chosen. Moreover, our results have been obtained for a simple model, which assumes that all interactions are represented by the Lennard-Jones potential. Therefore, the model is applicable only to monolayers formed by simple atomic adsorbates on also simple atomic crystals. Examples of such systems are the films formed by noble gases on the crystals of different noble gases. The formation of AT phase requires that the adsorbate atoms are considerably larger than the substrate atoms, so that experiments should be carried out using heavier noble gas as the adsorbate and lighter one as the substrate. We are not aware of any experimental studies for such systems. It is, of course, possible that the formation of AT phase may occur in other systems. For example, in monolayers of atomic adsorbates on metals, ionic crystals (e.g., NaCl, KCl) as well as on other crystals of square surface symmetry, such as MgO.

Acknowledgements This work has been supported by the EC under the grant No. MTDK-CT-2004-509249.

References

Abraham, F.F.: The phases of two-dimensional matter, their transitions, and solid-state stability: A perspective via computer simulation of simple atomic systems. Phys. Rep. **80**, 340–374 (1981)

Allen, R.E., Alldredge, G.P., de Wette, F.W.: Studies of vibrational surface modes. I. General formulation. Phys. Rev. B **4**, 1648–1660 (1971)

Antsygina, T.N., Poltavsky, I.I., Poltavskaya, M.I., Chishko, K.A.: Lattice dynamics and heat capacity of a two-dimensional monoatomic crystal on a substrate. Low Temp. Phys. **28**, 442–451 (2002)

Braun, J., Fuhrmann, D., Šiber, A., Gumhalter, B., Wöll, C.: Observation of a zone-center gap in the longitudinal mode of an adsorbate overlayer: Xenon on Cu(111). Phys. Rev. Lett. **80**, 125 (1998)

Bruch, L.W.: Zone-center gap in the frequency spectrum of a commensurate monolayer. Phys. Rev. B **37**, 6658–6662 (1988)

Bruch, L.W., Cole, M.W., Zaremba, E.: Physical Adsorption: Forces and Phenomena. Clarendon, Oxford (1997)

Bruch, L.W., Graham, A.P., Toennies, J.P.: Vibrations of the commensurate monolayer solid Xe/Pt(111). Mol. Phys. **95**, 579–585 (1998)

Bruch, L.W., Graham, A.P., Toennies, J.P.: The dispersion curves of the three phonon modes of xenon, krypton, and argon monolayers on the Pt(111) surface. J. Chem. Phys. **112**, 3314–3332 (2000)

Bruch, L.W., Diehl, R.D., Venables, J.A.: Progress in the measurement and modeling of physisorbed layers. Rev. Mod. Phys. **79**, 1381–1454 (2007)

Cardini, G., O'Shea, S.F.: Dynamics of a monolayer of nitrogen physisorbed on graphite. Surf. Sci. **154**, 231–253 (1985)

Dash, J.G.: Films on Solid Surfaces. Academic Press, New York (1975)

de Rouffignac, E., Alldrege, G.P., de Wette, F.W.: Dynamics of xenon-covered graphite slabs. Phys. Rev. B **24**, 6050–6059 (1981)

Gibson, K.D., Sibener, S.J.: New result in surface segregation of Ni–Cu binary alloys. Phys. Rev. Lett. **55**, 514–517 (1985)

Graham, A.P.: The low energy dynamics of adsorbates on metal surfaces investigated with helium atom scattering. Surf. Sci. Rep. **49**, 115–168 (2003)

Grünbaum, B., Shepard, G.C.: Tilings and Patterns. W.H. Freeman, New York (1987)

Hakim, T.M., Glyde, H.R., Chui, S.T.: Dynamics of xenon, krypton, and methane monolayers in registry with graphite. Phys. Rev. B **37**, 974–983 (1988)

Kim, H.-Y., Steele, W.A.: Computer-simulation study of the phase diagram of the CH_4 monolayer on graphite: Corrugation effects. Phys. Rev. B **45**, 6226–6233 (1992)

Leatherman, G.S., Diehl, R.D., Karimi, M., Vidali, G.: Epitaxial rotation of two-dimensional rare-gas lattices on Ag(111). Phys. Rev. B **56**, 6970–6974 (1997)

Mason, B.F., Williams, B.R.: Dispersion behavior in physisorbed Xe on KCl. Surf. Sci. **148**, L686–L690 (1984)

McTague, J.P., Novaco, A.D.: Substrate-induced strain and orientational ordering in adsorbed monolayers. Phys. Rev. B **19**, 5299–5306 (1979)

Novaco, A.D., McTague, J.P.: Orientational epitaxy? The orientational ordering of incommensurate structures. Phys. Rev. Lett. **38**, 1286–1289 (1977)

Patrykiejew, A., Sokołowski, S.: Order-disorder phase transitions in adsorbed films. I. Monolayer and bilayer films of square symmetry. J. Phys. Chem. C **111**, 15664–15676 (2007a)

Patrykiejew, A., Sokołowski, S.: Two-dimensional quasicrystals of decagonal order in one-component monolayer films. Phys. Rev. Lett. **99**, 156101-1–156101-4 (2007b)

Patrykiejew, A., Sokołowski, S., Binder, K.: Phase transitions in adsorbed layers formed on crystals of square and rectangular surface lattice. Surf. Sci. Rep. **37**, 207–344 (2000)

Patrykiejew, A., Sokołowski, S.: Patrykiewjew and Sokołowski reply. Phys. Rev. Lett. **100**, 019602 (2008)

Phillips, J.M., Bruch, L.W.: Quasiharmonic theory of two-dimensional crystals I. Lennard-Jones potentials, quantum corrected cell theory, and the quantum mechanical principle of corresponding states. Surf. Sci. **81**, 109–124 (1979)

Ramseyer, C., Hoang, P.N.M., Girardet, C.: Dynamics of commensurate ($N \times 2$; $N = 3, 4$) and incommensurate phases of an argon monolayer adsorbed on MgO(100). Surf. Sci. **265**, 293–304 (1992)

Rżysko, W., Patrykiejew, A., Sokołowski, S.: Incommensurate monolayers of Archimedean tiling on a square lattice. J. Phys., Condens. Matter **20**, 494226 (2008)

Schmiedeberg, M., Stark, H.: Comment on "Two-dimensional quasicrystals of decagonal order in one-component monolayer films". Phys. Rev. Lett. **100**, 019601 (2008)

Steele, W.A.: The physical interaction of gases with crystalline solids *1 I. Gas-solid energies and properties of isolated adsorbed atoms. Surf. Sci. **36**, 317–352 (1973)

Steele, W.A.: The Interaction of Gases with Solid Surfaces. Pergamon, Oxford (1974)